Reconstruction and analysis of a sub-Plinian fall deposit from the Astroni volcano (ca. 4100-3800 BP) in the Campi Flegrei area, Italy

Pfeiffer, T.[1,2], Costa, A.[2]

[1] Department of Earth Sciences, University of Aarhus, Denmark

[2]Osservatorio Vesuviano, Naples, Italy

Osservatorio Vesuviano – INGV
Via Diocleziano, 328
I-80124 Naples, Italy

Technical Report (2)
on the Scientific Collaboration OV-INGV Contracts Number:
909 (15-05-01)
1129 (26-06-03)
1134 (30-09-03)

Research Unit Responsible: Giovanni Macedonio

Reconstruction and analysis of a sub-Plinian fall deposit from the Astroni volcano (ca. 4100-3800 BP) in the Campi Flegrei area, Italy

Pfeiffer, T.[1,2], Costa, A. [2]

Abstract

A simple semi-analytical model presented in Pfeiffer et al.(2004) was applied to reconstruct the tephra deposit of a sub-Plinian phase (called Astroni 6, after Isaia et al., 2003) of an eruption of the Astroni volcano (ca. 4100-3800 BP) within the Campi Flegrei volcanic area in Italy.
In this model, the eruption column is assumed to act as a line source in order to neglect complex near/vent interactions. Therefore, the validity of the model is limited to the medium and far areas from the vent (beyond 10-20km), where the assumption of a line source can be justified. The distribution of the particles in the atmosphere is assumed to be only controlled by gravity, wind and eddy diffusion. The model accounts for two different types of particles (juvenile pumice and dense particles) within a used-defined range of granulometric classes.
The numerically calculated deposit was confronted with the observed deposit. Applying a least/squares method it was tried to optimize input variables such as distribution of particles and mass within the eruption column, wind and diffusion parameters by fitting the computed deposit with the observed one. A good correlation between the numerically calculated and the measured deposit could be achieved, although the quality of the input data is poor because of the lack of a sufficient number of distal sample points. Therefore, best fitting input parameters could not be well constrained and the presented results must be seen as a fairly rough estimate on eruption conditions only. In particular, the eruption column height predicted by the model is smaller than those presented by other authors (Isaia et al., 2003). However, the discrepancy is large enough to raise the question about the precision of other estimates as well.

1. Introduction

The Astroni volcano in the Campi Flegrei volcanic field, Italy, formed during a timely closely spaced series of eruptions dated between 4.1 and 4.8 ka during the last epoch of activity (4.8 - 3.8 ka) of the Campi Flegrei volcanic field in the southern Italy (Isaia et al., 2003). Its deposits include alternating layers of ballistic tephra, fall and flow deposits. Only one fall deposit has been recognized as the result of a sub-Plinian eruption column. It forms the main, basal part of the tephra unit named Astroni 6 by Isaia et al. (2003). This deposit is subject to the present study. The available field data for this study consist in 26 samples where the total thickness of the fall deposit is known or inferred as zero and analyses of component and grain-size distribution of 3 of

[1] Department of Earth Sciences, University of Aarhus, Denmark, Email: tpfeiffer@decadevolcano.net
[2] Osservatorio Vesuviano, V. Diocleziano, 328, Naples, Italy, Email: costa@ov.ingv.it.

these samples. Furthermore, qualitative descriptions of the deposit allow a rough estimate on the mass fraction between juvenile pumice, lithics, crystals and other components in the erupted tephra.
The numerical reconstruction was performed using a well-established two-dimensional diffusion-advection-sedimentation model that is described in detail in Pfeiffer et al. (2004) and is implemented as a modified version of the Fortran code "Hazmap" (Macedonio et al., 2003). However, a brief outline of the physical principles and its solution is presented in the following paragraphs.

2. The physical model

Far from the vent, the internal dynamic effects of eruption columns are neglected in order to describe the dispersion and sedimentation of tephra. Under this assumption, the motion of particles can be described sufficiently by wind transport, turbulent diffusion and settling of particles by gravity. As a consequence, the model is only valid sufficiently far from the vent, at a distance comparable to the eruption column height (e.g. Armienti et al., 1988) and its results are therefore only relevant in the medium-distal area, where tephra fall commonly is the major volcanic hazard.
The mass conservation equation for each class of particles with given settling velocity may be generally written as:

$$\frac{\partial C}{\partial t}+\frac{\partial (w_x C)}{\partial x}+\frac{\partial (w_y C)}{\partial y}+\frac{\partial (w_z C)}{\partial z}-\frac{\partial (v_{settl} C)}{\partial z}=K_x\frac{\partial^2 C}{\partial x^2}+K_y\frac{\partial^2 C}{\partial y^2}+K_z\frac{\partial^2 C}{\partial z^2}+S \qquad (1)$$

where C is the concentration of particles, t time, x, y, z spatial coordinates, w_i the wind field, K_i the eddy diffusion coefficients ($i = x, y, z$), $v_{settl} := v_s$ settling velocity and S a source function describing the influx of mass from the eruption column. Eq. (1) is valid for each class j of particles having a given settling velocity v_s.

2.1 Eruption column and vertical mass distribution

In this model, the eruption column acts as a vertical line source. Since this simplification is only valid far from the vent, the use of the model is limited to areas sufficiently far from the vent. The results from Macedonio et al. (1988) and Armienti et al. (1988) suggest that this critical distance is approximately given by the height of the eruption column itself. Since eq. (1) is linear in mass, an instantaneous release of the total mass from the eruption column can be assumed if wind and diffusion parameters do not change significantly with time. Variations of the eruption column with time are in this approach replaced by a time-averaged column.
To describe the vertical mass distribution in an eruption column, a modified version of the formula suggested by Suzuki (1983) is applied. It describes the vertical mass concentration uniformly for all particle classes as:

$$S(x,y,z,t)=S_0\left\{\left(1-\frac{z}{H}\right)\exp\left[A\left(\frac{z}{H}-1\right)\right]\right\}\delta(t-t_0)\delta(x-x_0)\delta(y-y_0) \qquad (2a)$$

where $S(z) := \{1\text{-}z/H \exp [A/(z/H\text{-}1]\}$ is the vertical mass distribution function, z the altitude in the eruption column, S_0 a normalization factor, H the maximum plume height, A a dimensionless parameter ("Suzuki coefficient") and δ is the Dirac's distribution (punctual and instantaneous release assumption). Eq. (2a) is considered a merely empirical description of the vertical mass

distribution within the eruption column with a purely geometric meaning. The value of A describes the vertical position of the maximum concentration relative to the maximum column height, located at (A-1)/A of the maximum plume height (Fig. 1a).
Theoretical and empirical observations on buoyant plumes (e.g. Morton et al., 1956; Sparks, 1986) show that the ratio H_B/H_T between the height of buoyancy of the plume H_B and its maximum height H_T is usually around 3/4. This is here accounted for by setting A=4 in eq. (2a). Instead of using A, a different parameter called λ is introduced:

$$S(z) = S_0 \left\{ \left(1 - \frac{z}{H}\right) \exp\left[A\left(\frac{z}{H} - 1\right)\right]\right\}^{\lambda} \qquad (2b)$$

The value of the parameter λ is a measure of how strongly the total mass is concentrated around the maximum concentration at H(A-1)/A (Fig. 1b). In this study, both factors were set at fixed values of 1.

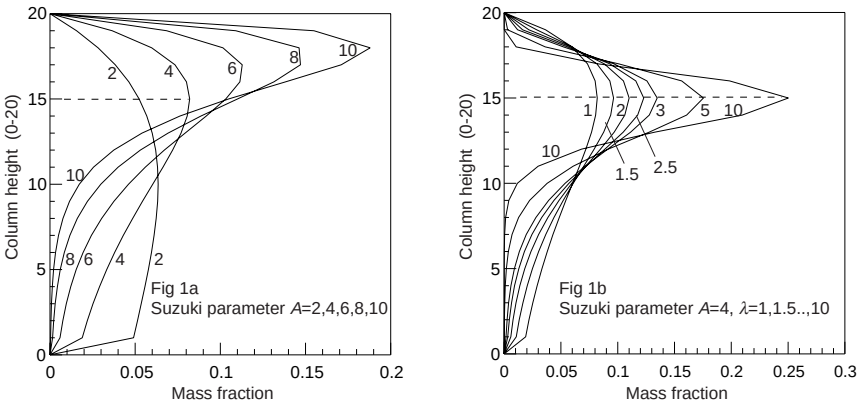

Fig. 1. Models describing the vertical mass distribution (here for a 20 km high eruption column) according to the modified formula of Suzuki (1983) (eq. 2a/b). The values of the Suzuki parameters A and l were varied between A=2, 4, 6, 8, 10 with l =1 (Fig. 1a) and l=1, 1.5, 2, 2.5, 3, 5, 10 with A=4 (Fig. 1b).

2.2. Atmospheric turbulent diffusion, wind translation and deposition

Following previous studies (e.g. Armienti et al., 1988), both vertical diffusion and wind components are usually of an order of magnitude smaller than the horizontal components and are therefore neglected in this model. In addition it is assumed:

(1) Eddy diffusion acts homogeneously in all horizontal directions, and thus $K_x=K_y := K$.

(2) The diffusion coefficient $K_{x,y}$ is constant. Horizontal wind components vary only with altitude z.

(3) Horizontal wind components are constant in time and within the horizontal domain. This assumption should hold for intermediate distances of the order of 50-100 km or more, but becomes increasingly wrong with large distances.

Under these additional assumptions, eq. (1) simplifies to:

$$\frac{\partial C}{\partial t} + \frac{\partial (w_x C)}{\partial x} + \frac{\partial (w_y C)}{\partial y} - \frac{\partial (v_{sett} C)}{\partial z} = K\frac{\partial^2 C}{\partial x^2} + K\frac{\partial^2 C}{\partial y^2} + S \qquad (3)$$

Analytical solutions of eq. (3) are available, if settling velocities and horizontal wind components can be assumed not dependent on z, which consist in a 2D-Gaussian solution (e.g. Pfeiffer et al.2004, Macedonio et al., 2004). It assumes that each class of particles (with the same settling velocity) has a Gaussian-shaped distribution in each horizontal layer at any time:

$$C(x,y,z,t) = \frac{C_0^*}{4\pi K t} \exp\left[-\frac{(x - x_c)^2 + (y - y_c)^2}{4Kt} \right] \quad (4)$$

where C_0* is a normalization factor and $x_c=w_x t$, $y_c=w_y t$ the center coordinates of the Gaussian wind-advected cloud. Eq.(4) is a solution of (3), but not sufficient to describe the whole tephra cloud with a given initial vertical mass distribution. Therefore, the 4-dimensional domain is split into thin horizontal layers that 'fall' to the ground together with the particles originally contained in a given initial vertical interval [z1; z2] at time t=0. A solution in the form of eq. (4) is then found for each layer. Since the whole treatment is done separately for each class of particles and no vertical diffusion and wind advection takes place, all particles falling from the same initial height remain at all times at the same altitude. While the center of each cloud is translated by wind, the cloud spreads horizontally due to diffusion and settles by gravity until it reaches the ground where it forms the deposit. For more details of the mathematical description of the model see Pfeiffer et al. (2004) and Macedonio et al. (2004).

2.3.Settling velocity of particles

Settling velocity of volcanic particles is a complex function of particle size, shape and density and depends also on density and viscosity of the surrounding air. Its value can only be computed approximately and relies heavily on empirical data. In this study, it is calculated for each size and component class at each altitude separately, according to Pfeiffer et al. (2004) and Pfeiffer (2003) who presented a set of formula that represents a best fit to available experimental data on pyroclastic particles.
Since particle settling velocity changes with altitude and Reynolds number, only particles with the same size, shape and density can be strictly regarded as belonging to one settling velocity class (for details see Pfeiffer et al., 2004). Particles with different densities that belong to a given settling velocity class at a given altitude can have different settling velocities at other altitudes, depending on their different Reynolds numbers. It is therefore better and more correct to treat each size class of each present component as a single settling velocity class, rather than simply dividing the bulk settling velocity spectrum (containing all components) at a given altitude, e.g. at sea level, into pure settling classes of (mixed component) particles, which has been a commonly used method in the past (e.g. Armienti et al., 1988).

3. Numerical modeling of the Astroni 6 basal fall deposit and input parameters

The numerical model outlined in the previous chapter was performed using a FORTRAN code called "fallout" (Version 57 as of 19 Oct. 2003, by T. Pfeiffer, unpublished), based on the program "Hazmap" by Macedonio et al. (2003). The program requires a number of input parameters, which either can be assigned fixed values or can be treated as free variables that are fitted to best match an observed deposit according to user-defined criteria. These parameters, together with the best-fitting results, are summarized in Tab. 2:

- Maximum height of the eruption column H. This parameter was allowed to vary between 8 and 30 km.
- Number and spacing of vertical source points to model the eruption column. In this study, 20 equally spaced source points were taken.
- Vertical mass distribution in the eruption column (cf. 2.1). Due to the very limited number of good input data, the factors A and λ in eq. (2) were not varied and fixed at A=1 and λ=1.
- Constant eddy diffusion coefficient K. This parameter was varied between 2000 and 7000 m^2/s.
- Total mass. It was found by best fitting the calculated with the measured deposit.
- Wind speed and direction at given levels. See respective chapter 3.2.
- Initial bulk component, particle density and grain-size spectrum of erupted tephra. See respective chapter 3.3.
- Average void fraction of deposit: since the measured deposit is given only as thickness data with no measured bulk deposit density values, this parameter is necessary for the program to calculate deposit thickness from the originally calculated mass-per-area-unit data. Considering the overall appearance of the deposit, a completely compacted deposit was assumed, i.e. void fraction was assumed to be 0%. The deposit volume (and hence, thickness) was calculated as the sum of all (density-dependent) volume contributions of each particle class depositing in each point on the ground.

3.1.Field data and fitting method

Fitting was performed on the published field data (Isaia et al., 2003) and other unpublished data collected by Orsi-Isaia team, using a least-square method comparing measured and calculated data. Because of the inherent limitation of the model to medium-range and far parts of a deposit, the available data from samples was weighted as follows: Sample points between 1 and 10 km from the vent were given progressively increasing weight from 0 to 1, while weight 1 was applied for all samples at distances greater than 10 km. In order to compensate for the lack of (vital) distal field data (the model is technically not valid at distances lower than about the eruption column height, i.e. 10-15 km), 8 data points were added manually, where field experience and intuition allows assuming that no tephra was deposited (although this procedure might be questionable, see discussion). Afterwards, all weights were renormalized. 28 data of deposit thickness and a total of 5 (nr. of points) X 11 (measured size classes) = 55 grain-size data were used (but only for two points component analysis data were available). Both data sets were given equal weight in the fitting procedure.

3.2.Bulk component and grain-size spectrum of erupted tephra

The initial bulk component and grain-size composition of erupted tephra is a crucial requirement for the model. However, to find a reasonably well constrained fit, measured grain-size and component data in many more than 3 sampling points must be available. In addition, only in two sample points (indicated as A-319/A-366 by Isaia's team) a component analysis was available as well. In this sample, around 95 wt% of the deposit consists of juvenile pumice. The rest is composed of lithic fragments, crystals and dens glass. This and the qualitative description of the deposit by Isaia et al. (2003) suggest that in fact, most of the deposit is composed by pumice. However, the typically small grain-sizes of the other components will result in their preferred

deposition at relatively far distances and the proximity of the analyzed part of the deposit do not exclude that a significant amount of fine particles is present in the bulk erupted tephra. Further, this sampling point as well as the description of the deposit belong to its proximal part. It is a reasonable assumption applied to most Plinian and subplinian eruptions that a significant amount of material is fine-grained. For this reason, in this study, two components were used: pumice a class of dense particles of unspecified nature, with their relative weight percentage varied between 60 and 90 wt% (for the pumice component).
In lack of data of the density of each size class of the two components, density values for the pumice component were assumed to be similar to measured ones for the Vesuvius 79 AD eruption – the White Pumice deposit - (Macedonio et al., 1988). The applied values are given in Tab. 1. For the fine fraction (lithics, crystals and dense glass shards), uniform density of 2500 kg/m^3 was applied. The logarithmically expressed grain-size distribution for each component was assumed to be Gaussian with a mean and standard deviation of logarithmic grain-size, which were varied independently for both components between $-4 < \mu(\Phi)$ (Gaussian mean) $< +4$ and $1 < \sigma(\Phi)$ (Gaussian standard deviation) < 3. The resulting grain-size spectra of erupted bulk mass are given in Fig. 2 with the resulting distributions of settling velocity shown in Fig. 3.

Tab. 1. Grain-size dependant density of juvenile pumice as used in the model. Data modified after Macedonio et al (1988), who report density data of juvenile pumice from Vesuvius 79 A.D. Gray Pumice deposit.

Φ	**Density**
<= -1.5	650 kg/m^3
-0.5	900 kg/m^3
0.5	1150 kg/m^3
1.5	1430 kg/m^3
2.5	1720 kg/m^3
3.5	2010 kg/m^3
>= 4	2300 kg/m^3

3.3. Wind

Vertical wind components are neglected in the model because they are on an average of an order of magnitude smaller than horizontal components. Two different wind models (W1 and W2) were applied to the reconstruction of the Astroni 6 fall-out tephra. The used wind profiles are given in Fig. 4.
In the first model W1, wind speeds from a measured wind profile for southern Italy (summer wind profile from Cornell et al., 1983) are scaled with a factor found by best fitting, whereas all wind vectors have the same direction, which is found by best fitting.
In the second wind model (W2), a generic wind profile is found by best fitting. It assumes linearly increasing wind speeds from 4 m/s on the ground to a variable, best-fitted wind maximum wind speed at the tropopause level, here taken at 10.8 km altitude, and a second best fitted constant wind speed above 15 km altitude. Wind speeds at intermediate levels between 10.8 and 15 km are linearly interpolated. As in W1, all wind directions are in the same direction. This wind model has the ability to produces wind profiles that have the characteristics of the autumn, winter and spring profiles of the region, where the wind direction below and above the tropopause is roughly constant (Cornell, 1983).

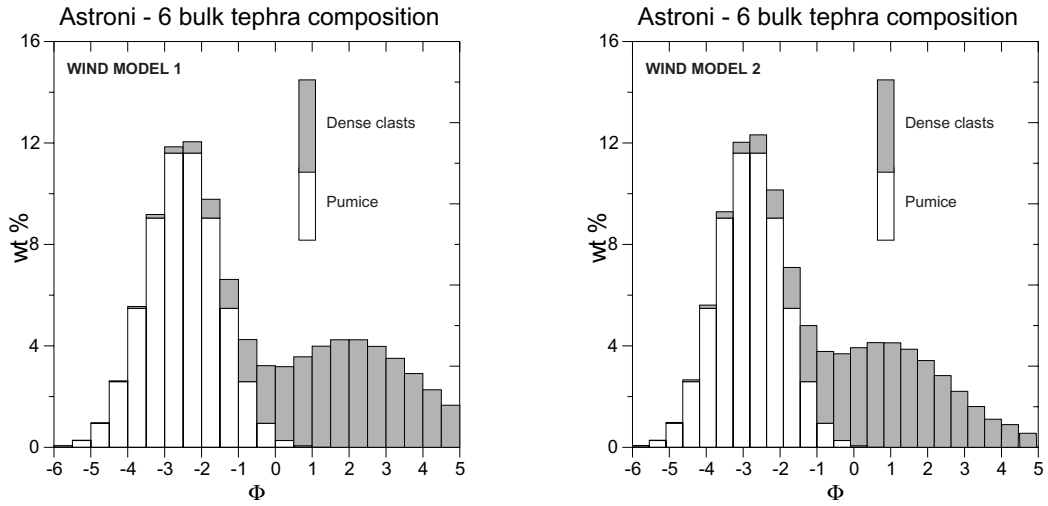

Fig. 2. Grain-size and component distribution in model bulk eruption mass.

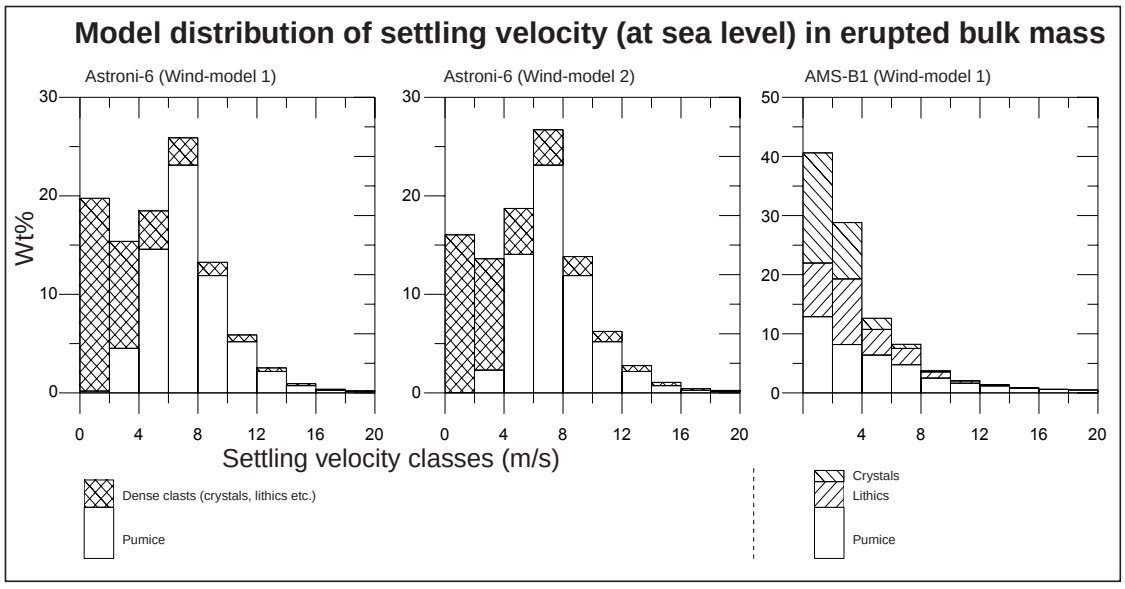

Fig. 3. Model distribution of settling velocity (at sea level) in erupted bulk mass for both runs of the Astroni-6 fall layer reconstruction. For comparison, the corresponding spectrum of the reconstruction of the Agnano-Monte-Spina fall-layer B1 (using wind-model 1) from Pfeiffer (2004b) is shown as well. Settling velocity was calculated as in Pfeiffer et al. (2004).

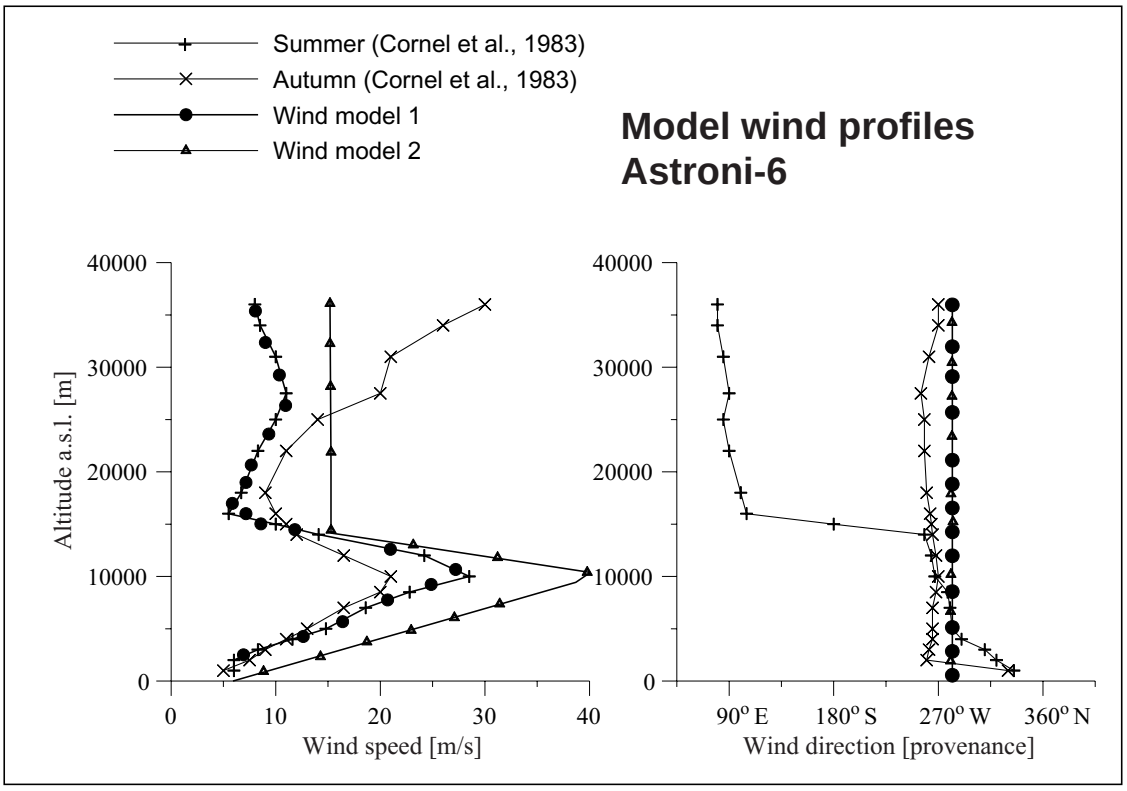

Fig. 4. Wind profiles used in the two model reconstructions. For comparison, the statistical wind profiles for summer and autumn winds in the S-Italian region are shown (from Cornell et al., 1983).

4. Results and Discussion

Both reconstructions using the two different wind models give very similar results and in both cases the numerically calculated deposits are in reasonably good agreement with the measured one (Tab. 3). The results and used parameters are summarized in Tab. 2-3 and Figs. 2-6. However, the overall quality of the fitting represented by the CHI-square method is not very good, most likely due to the limited number of good data. This becomes clear when the difference between the two reconstructions are examined in detail. In both cases, the best-fitting eruption column is only around 10 km high, i.e. high wind levels are not significant. The initial grain-size compositions of the erupted tephra as well as diffusion coefficients are similar. A significant difference is that the first reconstruction using WM1 uses overall lower wind speeds but applies a higher eruption column, whereas WM2 has higher wind speeds and a lower eruption column. Both parameters are strongly correlated and the differences are subtle (Pfeiffer et al., 2004) and only good field data allow resolving the differences produced by opposing pairs such as high column/ low wind speeds and low column/ high wind speeds.

Both calculated deposits are equally good when compared to the real deposit. The different values of the input parameters can thus be seen as a measure of its uncertainty, which is in large part due to the limited data available, but this reflects a typical case and is therefore important.

A problem for the reconstruction using the present model was that most data points were relatively close to the vent and could only be used at if given low relative weights; on the other hand, while the few data points at distances of 10 or more km from the vent were weighted more heavily and are thus largely “responsible” for the results. In addition, 8 artificial points were added manually, where it is assumed that no or extremely little tephra was deposited. This might

be a source of underestimating the mass and eruption column, since it might well be possible, that a larger portion of the erupted mass was fine-grained, producing a thin deposit that however is not preserved today. As overall result, the estimates of parameters such as wind, column height and total mass produced by the model should be considered affected by a large error.

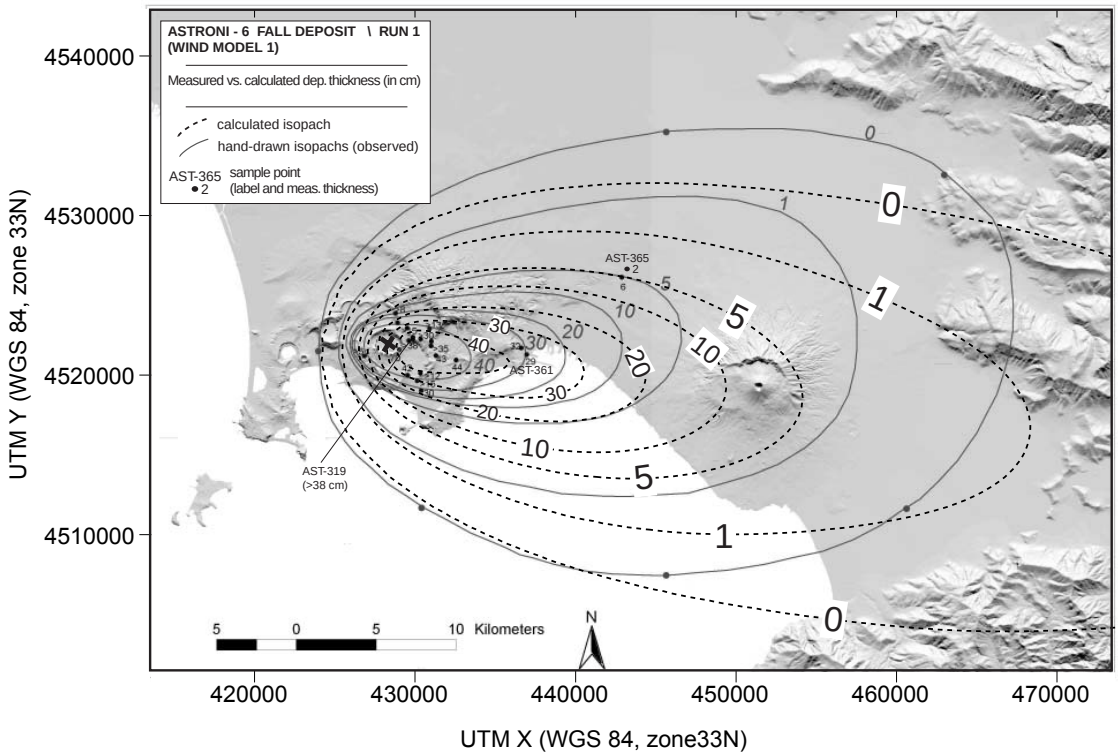

Fig. 5. Calculated (dotted lines) and isopachs inferred from measured deposit thickness on ground (from Isaia et al., 2003) of the Astroni-6 fall deposit in cm. Only the results of the reconstruction using wind model 1 are shown, because the other wind model produces near identical isopachs. Note that the most available data points (dots) are within 10 km of the vent area (cross) and thus not much informative for this model. The calculated deposit extends further to the E than inferred from available ground data.

Maximum eruption column heights predicted by the model are around 8-12 km, significantly lower than the estimate of around 20 km by Isaia et al. (2003), or around 15 km if estimated by the method of Carey and Sparks (1986). As pointed out, the lack of more distal data limits the credibility of the present result. High eruption columns would produce large amounts of distal tephra fall and in the present case, it is difficult to decide whether such a distal tephra deposit has gone undetected, possibly because it has long since eroded.

The reconstructed wind direction is regarded as a more reliable parameter, since it can be strongly constrained by best fitting using a wide range of other parameters. The main distribution axis can be defined at a easterly direction with wind speed profiles similar to typically observed ones today. Diffusion coefficients assume best-fitting values between 5000-7000 m^2/s, which can be seen as the upper limit of realistic values for a simulated tephra deposit dispersed over about 50 km horizontal distance along the wind axis.

The mass estimates of the model can be seen as an estimate of the documented mass of the deposit on the ground only and are at around $4\text{-}5 \times 10^{10}$ kg with an uncertainty of around 20-30% due to the unknown void fraction of the deposit (here, a compacted deposit was assumed; if void volume is still present the mass required to produce the same deposit would be accordingly

lower). The mass estimate is in agreement with that estimated by Isaia et al. (2003) who found a mass associated with the fall deopsits of about 1/5th of the total deposit ($2.5x10^{11}$ kg) including the Plinian fall deposit and phreatomagmatic deposits following the Plinian phase. Since the calculated isopachs of the model fit well to the available thickness data on the ground (Fig. 5), the presented mass estimate is a good value of the *preserved* deposit in the study area, but might exclude a significant portion of distal tephra.
Since the eruption column of the model is not very high, even a fairly good agreement of calculated and measured data in the near-vent area is achieved (Fig. 5). A test has been made to exclude all data points at distances lower than 5 km as well as the 8 manually-added points where the deposit is assumed to be zero (i.e. where no tephra has fallen). In this case, only 4 samples including two with grain-size information are used and it is immediately clear that good fitting with 4 data points is not possible at all. However, the results produced by this method are nevertheless similar to the presented results, where also the other, but questionable data are included.

Tab. 2. Input parameters and best-fitting values.

Run	**Wind model 1**	**Wind model 2**
Parameter		
Number of Φ-classes	22	22
Nr. of vertical source points	20	20
Total mass	$4.1x10^{10}$ kg	$4.1x10^{10}$ kg
Column height	12 km	9 km
Suzuki para. λ/A=4 (fixed)	1/1	1/1
Pumice bulk grain-size		
Gaussian mean μ (Φ)	-2.5	-2.5
Standard deviation σ (Φ)	1.0	1.0
Wt %	60	60
Dense particles bulk grain size (lithic fragments, crystals, glass shards)		
Gaussian mean μ (Φ)	2.0	2.0
Standard deviation σ (Φ)	2.0	2.0
Wt %	40	40
Other parameter		
Diffusion coefficient	5,500 m^2/s	7,000 m^2/s
Wind direction <11 km	278° W	278° W
Max. w. speed at 11 km	29 m/s	40 m/s
Max. eruption column height	12 km	
Fitting results		
$\chi^2_{tot.}$ (total deposit)	32.9	30.1
$\chi^2_{grain\text{-}size}$ (grain-size spectra)	162.7	166.3
Weighted $\chi^2 = \chi^2_{tot.} + \chi^2_{grain\text{-}size}$	195.7	196.4
Degrees of freedom n_F (number data – variables)	(26+3X11) 59-11= 48	(28+5X11) 83-12=61
Reduced $\chi^2_{red} = \chi^2 / n_F$	4.08	3.22

5. Conclusion

The application of the Hazmap model to the Astroni 6 fall deposit showed that the model is able to produce a credible, or at least physically reasonable fit, even in cases where few data are available. With few good data (less than ca.10 points at distances greater than the eruption

column height) estimates produced by the model should be considered affected by a considerable error. In the specific case of the Astroni 6 fall deposit, the model results suggests that the eruption was of lower intensity than estimated by field observations and other models (Isaia et al., 2003). Whether this might be true or not, it is emphasized that even a relatively small eruption (less than 10^{11} kg of erupted tephra, or around 400 million m^3 DRE –around 20 times the erupted material of Mt. Etna's last (explosive) eruption in 2002/2003 – can produce a significant tephra layer that would have a severe impact on today's infrastructure in the Napoletanean area.

Tab. 3. Comparison of measured and calculated deposit thickness data

Sample nr as in Isaia et al. (2003)	Distance from vent (km)	Observed deposit thickness (cm)	Calculated thickness (cm)	
			Wind model 1	Wind model 2
319	1.6	>38	35	34
361	8.7	29	26	27
365	15.5	2	2.6	2.7
308	3.1	43	33	32
313	2.0	>8	12	11
316	4.4	44	31	31
152	2.3	42	20	19
325	2.0	>30	34	33
327	1.7	>5	5.9	5.3
340	15.2	6	3.8	3.9
344	1.5	>15	28	27
346	3.6	30	15	13
348	0.8	>70	37	36
350	8.3	32	26	27
305	2.7	>35	34	33
362	2.7	>13	28	26
363	2.0	>15	29	27
364	2.7	>12	25	24
m. a.*	9.4	0 *	0.02	0.01
m. a.	22	0 *	0.01	0.00
m. a.	36	0 *	0.02	0.02
m. a.	39	0 *	0.55	0.57
m. a.	34	0 *	0.78	0.82
m. a.	78	0 *	0.00	0.00
m. a.	10	0 *	0.05	0.04
m. a.	4.4	0 *	0.10	0.06

* m. a.: manually added points with inferred absence of tephra deposit

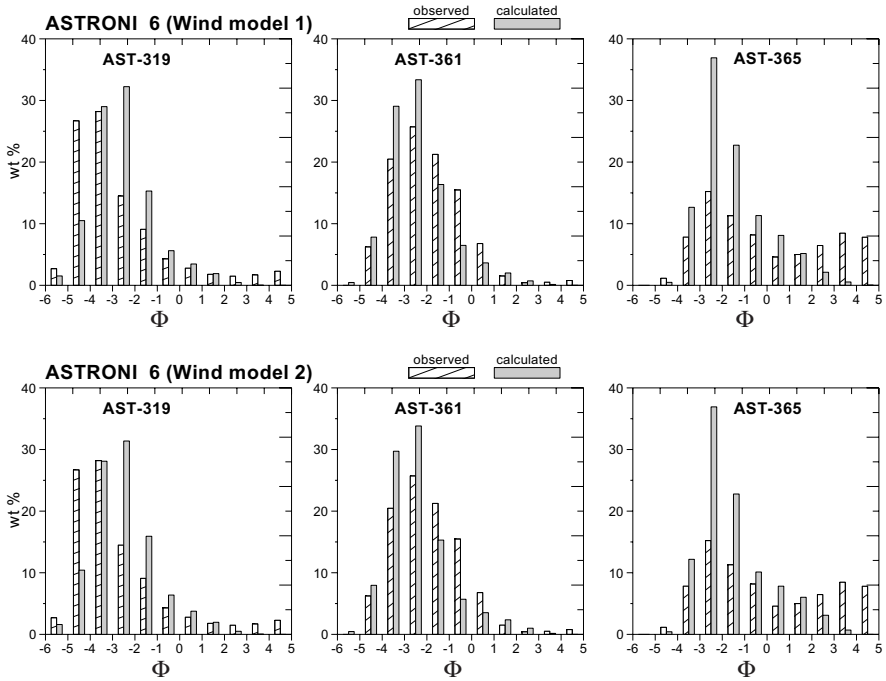

Fig. 6. Calculated and measured grain-size distribution of the Astroni-6 fall deposit on ground in three available sample points. Laboratory data from R. Isaia (personal information). Only sample point AST-365 is sufficiently far from the vent

Acknoledgements

Roberto Isaia and Francesco Dell'Erba are acknowledged for providing field data and site coordinates.

References

Armienti, P., Macedonio, G., Pareschi, M.T. (1988). A Numerical Model for Simulation of Tephra Transport and Deposition: Application to May 18, 1980, Mount St. Helens Eruption - Journal of Geophysical Research 93, p.6463-6476.

Carey, S. and Sparks, R.S.J. (1986). Quantitative models of the fallout and dispersal of tephra from volcanic eruption columns. Bulletin of Volcanology, 48 (2/3), 127-141.

Cornell, W., Carey, S., Sigurdsson, H. (1983). Computer simulation and transport of the Campanian Y-5 ash, Journal of Volcanology and Geothermal Research, 17, 89-109.

De Vita, S., Orsi, G., Civetta, L., Carandente A., D'Antonio, M., Deino, A., di Cesare, T., Fisher, R.V., Isaia, R., Marotta, E., Necco, A., Ort, M.H., Pappalardo, L., Piochi, M., Southon, J. (1999). The Agnano-Monte Spina eruption (4100 years B.P.) in the restless Campi Flegrei caldera. Journal of Volcanology and Geothermal Research, 91, p. 269-301.

Isaia, R., D'Antonio, M., Dell'Erba, F., Di Vito, M., Orsi, G. (2003) The Astroni volcano: the only example of closely spaced eruptions in the same vent area during the recent history of the Campi Flegrei caldera (Italy), Journal of Volcanology and Geothermal Research, 2035, p. 1-22.

Macedonio, G., Pareschi, M.T., Santacroce, R. (1988). A Numerical Simulation of the Plinian Fall Phase of 79 A.D. Eruption of Vesuvius - Journal of Geophysical Research, 93, p. 817-827.

Macedonio, G., Costa A., Longo, A. (2004). Computer model of volcanic ash fall-out sustained columns and hazard assessment. Accepted for the pubblication on Computer & Geosciences.

Pfeiffer, T. (2003) Numeric reconstruction of tephra-fall deposits from the 18 august and 16/17 September 1992 eruptions of Crater Peak, Mt. Spurr volcano, Alaska, in: Two catastrophic volcanic eruptions in the Mediterranean – Santorini 1645 B.C. and Vesuvius 79 A.D., Ph.D. thesis, Dep. of Earth Sciences, University of Aarhus, Denmark, 141-183.

Pfeiffer, T., Costa A., Macedonio, G. (2004) A model for the numerical reconstruction of tephra-fall deposits, Journal of Volcanology and Geothermal Research, in press.

Suzuki, T. (1983) A theoretical model for dispersion of tephra. In: Volcanism: Physics and Tectonics, edited by D. Shimozuru and I. Yokoyama, pp. 95-113, Arc, Tokyo.